

An Apparatus for the Electrodynamic Containment of Charged Macroparticles

A. Williams, R. Melbourne, L. Maleki, G. Janik, and J. Prestage
Communications Systems Research Section

The dynamic motion of the ions contained in the trapped $^{199}\text{Hg}^+$ frequency standard contributes to the stability of the standard. In order to study these dynamics, a macroscopic analog of the $^{199}\text{Hg}^+$ trap is constructed. Containment of micron-sized particles in this trap allows direct visual observation of the particles' motion. Influenced by the confining fields and their own Coulomb repulsion, the particles can form stable arrays.

I. Introduction

JPL is involved in the research and development of new technologies which surpass the stability of standards such as the hydrogen maser. One of the technologies under development in the frequency standards laboratory (FSL) at JPL is the trapped mercury ion frequency standard.

Like the cesium beam, hydrogen maser, and other atomic frequency sources, the trapped ion standard is based on an atomic transition. When an atom makes a transition from an energy level E_1 to a lower level E_2 ,

a photon of frequency $\nu = (E_1 - E_2)/h$ (h being Planck's constant) is emitted. Thus, an atomic transition creates a frequency source. However, the atomic energy levels are shifted, split, or broadened when disturbed by electric or magnetic fields, spin-exchange collisions, etc. Therefore, to obtain very stable frequency standards, it is desirable to protect the atoms from such offenders. This is the motivation for holding the atoms in an electromagnetic trap in a very high vacuum [1].

This article describes the construction and operation of a macroparticle trap which will be used to study the

dynamics of charged particles confined in a trap and the parameters that influence the details of their motion. Since the trap allows the confinement of micron-sized particles, a direct visual observation of the dynamics in the trap is possible. In particular, phenomena such as cooling, crystallization [2], and evaporation of confined particles become directly observable.

The versatility of this experimental environment permits the testing of various traps; the construction of a novel linear trap [3] for confinement of micron-sized particles will enable the first study of the dynamics of charged particles in this trap geometry. Insight into the motion of charged particles confined in such a linear trap will allow the modeling of the dynamics of ions in the linear trapped $^{199}\text{Hg}^+$ frequency standard.

The magnitude of variation in the second-order Doppler shift comprises the largest practical limit on the frequency stability achievable with a trapped ion frequency standard [3]. Since the shift is due to the motion of ions in the trap, a model of the ion dynamics in the $^{199}\text{Hg}^+$ trap will aid the determination of parameters which minimize variation in the second-order Doppler shift.

The organization of the article is as follows. First, in Section II, the theory of trapping charged particles in a radio frequency (RF) trap is discussed. The details and results of macroparticle trap research are described in Section III. Results obtained with a hyperbolic trap are given in Section IV, and a look ahead to other capabilities of the system is presented in Section V.

II. Trapping Theory

The type of trap that has been often employed for frequency-standard applications is the Paul trap, one type of RF trap. It consists of three hyperbolic electrodes: two endcaps, which are a hyperboloid of two sheets, and a ring electrode, which is a hyperboloid of one sheet (Fig. 1). The trap, when assembled with the ring between the two endcaps, has characteristic dimensions in cylindrical coordinates of z_0 , half the distance between the endcaps, and r_0 (usually set to be equal to $\sqrt{2} \cdot z_0$), half the distance across the ring. See Fig. 2 for a cross-sectional view of the assembled trap.

To operate the trap, an AC voltage in series with a DC voltage is applied between the ring and the endcaps (Fig. 2), which produces a potential

$$\phi(r, z) = \frac{V_{\text{DC}} - V_{\text{AC}} \cos \Omega t}{z_0^2} \left(z^2 - \frac{r^2}{2} \right) \quad (1)$$

inside the trap [2]. From this expression for the potential the electric field $\mathbf{E} = -\nabla\phi$ is easily obtained:

$$\mathbf{E} = \frac{(-V_{\text{DC}} + V_{\text{AC}} \cos \Omega t)}{z_0^2} (2z\hat{z} - \hat{r}) \quad (2)$$

It is clear that the field intensities E_z and E_r (and hence the forces F_z and F_r) vary linearly with z and r , respectively, and that the electric field \mathbf{E} is zero at the center, or node ($r = z = 0$) of the trap. It is also seen that the field intensity in the z direction is twice as strong as that in the r direction and has opposite sign. This negative sign shows that when the confining fields point toward the node in one direction, they point away in the other.

It may not be immediately obvious that an alternating potential should stably confine charged particles. The "secret" lies in the fact that the forces toward the node increase with distance away from the node. Suppose that in one half-cycle of the potential, the force on a particle is away from the node (Fig. 3). At the second half of the cycle, the particle is situated at a point of stronger field than where it started. Now the force is not only directed toward the node, it is larger in magnitude, thus leaving the particle closer to the node than it started. It should now be clear that over one period of the trapping potential, the net effect is to move the particle nearer to the node.

Stable confinement occurs in a region dependent on the charge-to-mass ratio of the particles, V_{AC} , V_{DC} , and Ω . When the system is operated with V_{DC} set to zero, the limit of stable containment is given by [2]

$$\left(\frac{e}{m} \right) \left(\frac{V_{\text{AC}}}{z_0^2} \right) \left(\frac{1}{\Omega^2} \right) - 0.908 < 0 \quad (3)$$

Thus, the charge-to-mass ratio can be determined by exploring the boundary of the stability region, where the particle is no longer trapped. Either V_{AC} or Ω is held constant and the other varied in order to find the boundary of stable operation. This experimentally determined value can then be substituted into Eq. (3) in order to solve for the charge-to-mass ratio.

III. The Macroparticle Trap

In 1959 the first visual observations of macroparticles in a Paul trap were made by Wuerker and his co-workers [2]. These investigations revealed interesting dynamic behavior when many particles were held in the trap—influenced by both the confining fields of the trap and their own Coulomb repulsion, the particles formed a stable array (Fig. 4). When the driving frequency of the trap was increased, the crystal “melted” and the particles underwent random motion in the trap. If the frequency was subsequently decreased, the particles would once again take up their stable array.

The first version of the JPL macroparticle trap consists of a hyperbolic electrode configuration with $r_0 = 1.9$ cm. Alumina powder (particle size nominally $5\text{ }\mu\text{m}$) is loaded into a small basket of stainless wire mesh. The basket is suspended from a Sonalert piezoelectric beeper which, when activated, shakes the basket and causes a fine mist of powder to fall through the mesh. This beeper-basket assembly is suspended above the trap, and the particles fall into the trap through a hole in the top endcap (Fig. 5). It is also possible to release particles from the basket without using the beeper by causing a discharge around the basket.

The entire trapping apparatus is mounted inside a custom vacuum chamber which has electrical feedthroughs on its bottom flange, a viewport for viewing in the r - z plane, two illumination windows perpendicular to the viewport, and a vacuum port. A mechanical pump evacuates the chamber to a pressure of about 5 mtorr. While the trap is operated primarily in this pressure regime, operation with pressures as high as 200 mtorr has also been carried out. The particles may be illuminated by any light source with sufficient power to make them visible; this particular system has been illuminated by a 0.5-mW helium-neon laser, a 15-mW argon ion laser, and a 300-mW dye laser. A Bausch and Lomb microscope with magnification 20 \times completes the viewing apparatus.

The 5-micron alumina particles have enough static charge to be trapped readily by the potential generated with $V_{AC} \approx 300$ volts at frequency $\Omega = 2\pi 60$ Hz. The trapping potential can thus be conveniently derived from ordinary wall power (110 V, 60 Hz) passed through a variac and a step-up transformer. By adjusting the variac, the RF potential can be chosen to be any value between 0 and 440 V. The DC voltage (V_{DC}) in series with the AC voltage is set to zero, and the bottom endcap is grounded. There

is also a DC voltage (V_g) which can be applied to the top endcap in order to counteract the gravitational pull on the particles (Fig 2).

With this system particles are readily trapped when the pressure in the vacuum chamber is lower than about 200 mtorr. Often both positively and negatively charged particles are trapped. The sign of the DC potential V_g applied to the top electrode of the trap allows the determination of the sign of the charge of the trapped particles.

IV. Results

Operating the trap in this way reveals behavior similar to that seen by earlier experimenters. Up to about 50 particles have been trapped by this system. Often both positively and negatively charged particles are contained. In the many-particle case, a crystal formation centered on the node and outlining the trapping fields is seen when V_g cancelled the weight of the particles (Fig. 6). The 60-Hz micromotion of the particles is seen to decrease in amplitude, as it should, when the particles are nearer to the node. With $V_g = 0$, the particles are pulled by gravity into the bottom of the trapping potential still in their crystalline formation. By adjusting the trapping potentials, the crystal can be broken and reformed. The particles have a wide range of charge-to-mass ratios, which can be approximately determined from the potential V_g necessary to counteract the gravitational force, on the order of 10^{-3} °C/kg. Those particles whose low charge-to-mass ratios cause them to locate themselves on the lower region of the particle cloud and can be ejected from the trap by varying V_g .

V. Other Capabilities of the System

Since $\Omega/2\pi$ is fixed at 60 Hz in this system, the charge-to-mass ratio of the particles can also be determined by measuring the maximum V_{AC} for stable confinement and using this measured value in Eq. (3):

$$\frac{e}{m} = 0.908 \left(\frac{(1.9 \text{ cm})^2 (2\pi \cdot 60 \text{ Hz})^2}{4V_{AC}^{\max}} \right) \quad (4)$$

By replacing the hyperbolic electrodes with any other suitably sized electrode configuration, the motion of charged particles in novel trap geometries can be studied with this system. The linear trap previously mentioned

has been implemented in the macroparticle system in this way, allowing visual study of the particle motion associated with the linear trapped $^{199}\text{Hg}^+$ frequency standard. A thorough study of the dynamics of particles in the linear trap is currently under way.

Since any dustlike or aerosol material with appropriate charge-to-mass ratio can be trapped in this system, a multitude of experiments on various substances are possible. For example, there are plans to operate the system at 0°C so that ice particles can be studied; such an investigation has significant application to atmospheric physics. A version of the system suitable for installation on a spacecraft could trap cosmic dust, which could subsequently be

irradiated with laser light for spectroscopic study of this material.

The physics of many-particle systems can also be readily studied with use of a macroparticle trap because the number of particles in the trap can be increased (by activating the beeper) or decreased (by ejecting those particles with extreme charge-to-mass ratios). The micro-motion of the particles and the form of the crystal may be observed as the crystal is cooled by viscous drag or heated by increasing V_{AC} . Quantitative measurements on the phenomena of crystallization and melting as functions of number of particles and particle energy help to describe the nature of several-particle systems.

References

- [1] L. Maleki, J. D. Prestage, and G. J. Dick, "Atomic Frequency Standards for Ultra-High-Frequency Stability," *TDA Progress Report 42-91*, vol. July-September 1987, Jet Propulsion Laboratory, Pasadena, California, pp. 67-72, November 15, 1987.
- [2] R. F. Wuerker, H. Shelton, and R. V. Langmuir, "Electrodynamic Containment of Charged Particles," *J. App. Phys.*, vol. 30, pp. 342-349, March 1959.
- [3] J. D. Prestage, G. J. Dick, and L. Maleki, "New Ion Trap for Frequency Standard Applications," *Proc. 20th Ann. PTTI Meeting*, pp. 305-311, 1988.

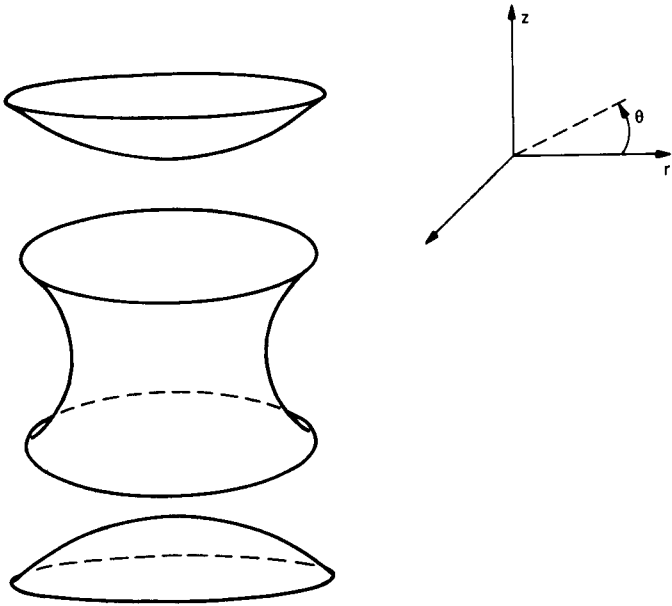


Fig. 1. The hyperbolic electrodes of a Paul trap.

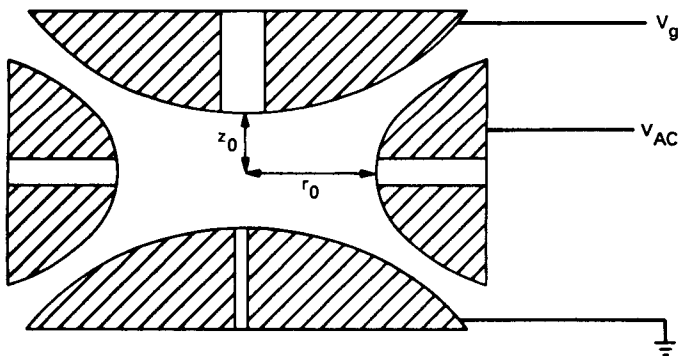
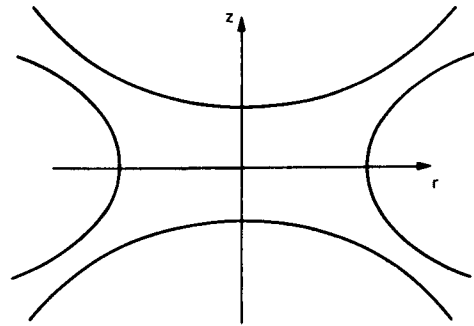


Fig. 2. Cross-sectional view of a Paul trap.

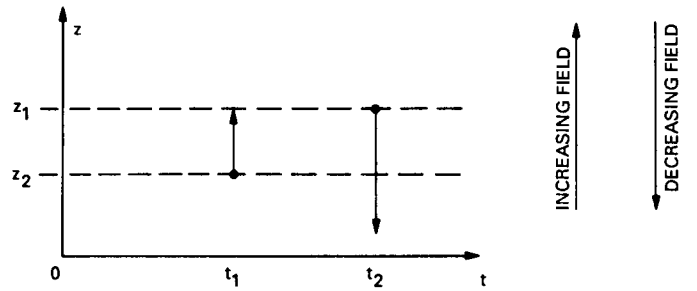


Fig. 3. One period of the AC trapping potential forces a particle toward the node ($r = z = 0$).

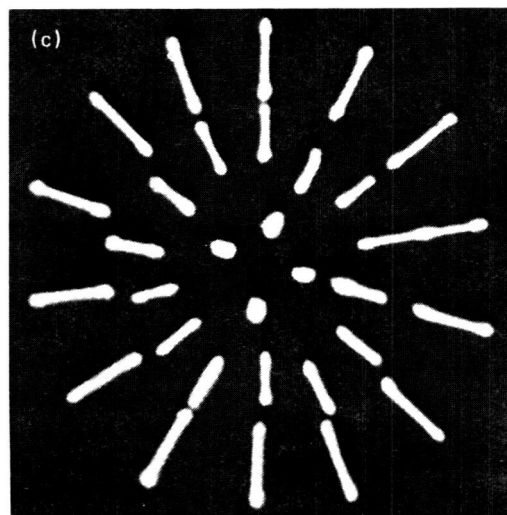
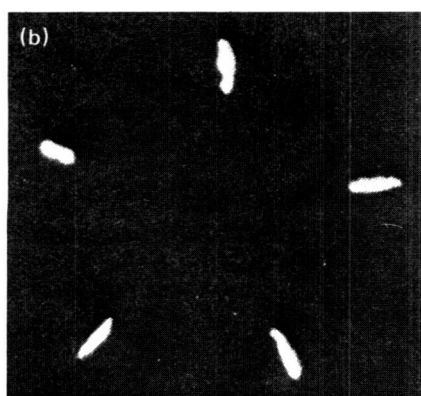
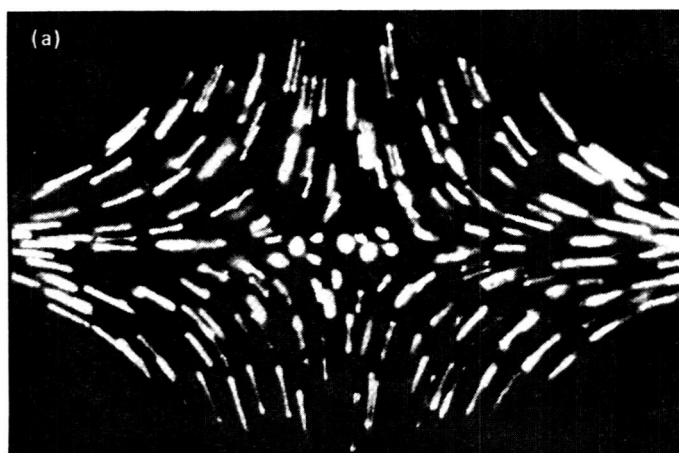


Fig. 4. Results of early work in macroparticle traps from [2], showing crystalline formations: (a) about 100 particles viewed in the r - z plane, (b) 5 particles viewed in the r - θ plane, and (c) 32 particles viewed in the r - θ plane.

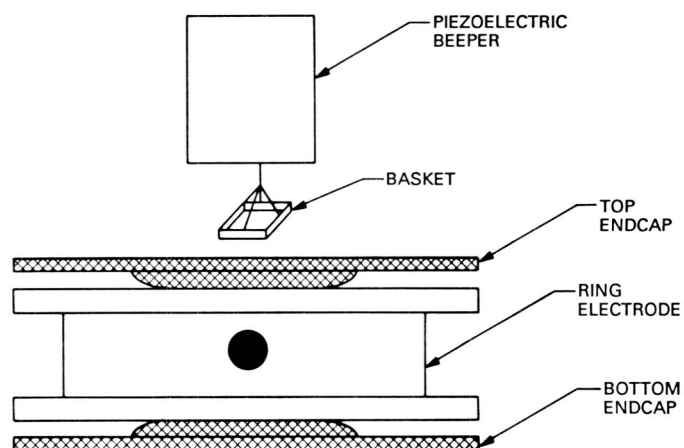


Fig. 5. Diagram of the present macroparticle introduction system, showing the beeper-basket assembly used for introduction through the top endcap.

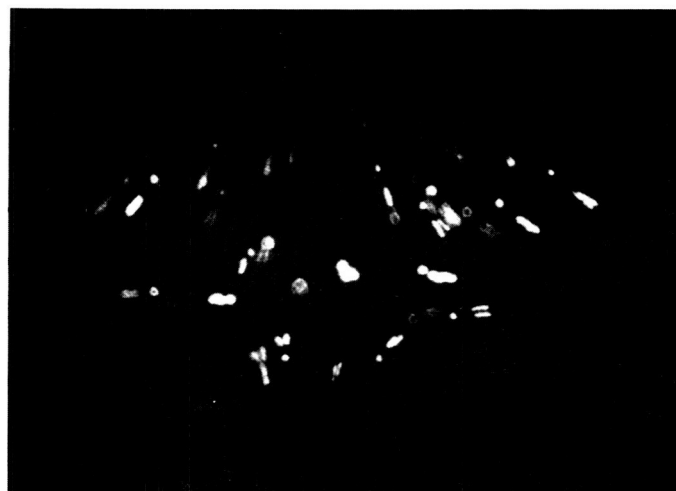


Fig. 6. An r - z photograph of about 45 alumina particles in the trap described in this article.